

Article

Extraction of Aluminum and Iron Ions from Coal Gangue by Acid Leaching and Kinetic Analyses

Deshun Kong^{1,2}, Zihan Zhou¹, Rongli Jiang^{1,*}, Shuojiang Song^{1,2}, Shan Feng² and Minglei Lian²

¹ School of Chemical Engineering and Technology, China University of Mining and Technology, Xuzhou 221016, China; LB19040009@cumt.edu.cn (D.K.); TB19040017B2@cumt.edu.cn (Z.Z.); LB20040020@cumt.edu.cn (S.S.)

² Guizhou Provincial Key Laboratory of Coal Clean Utilization, School of Chemistry and Materials Engineering, Liupanshui Normal University, Liupanshui 553004, China; 20132013071@cqu.edu.cn (S.F.); feiyuhu2003@126.com (M.L.)

* Correspondence: ronglij@cumt.edu.cn

Abstract: Extracting valuable elements from coal gangue is an important method for the utilization of coal gangue. In order to obtain the suitable technological conditions and the acid leaching kinetic model of leaching aluminum and iron ions from high-iron and low-aluminum coal gangue, the effects of calcination temperature, calcination time, and acid types on the leaching results of aluminum and iron ions are studied. The results show that when the gangue is calcined at 675 °C for 1 h, then the calcined gangue powder is leached by 6 mol/L hydrochloric acid at 93 °C for 4 h, the leaching ratio of iron ions is more than 90%, and that of aluminum ions is more than 60%. Furthermore, the acid leaching kinetic equations at 30 °C, 50 °C, 70 °C, and 90 °C are studied by three kinetic models, and the apparent activation energies of the reactions are calculated by the Arrhenius formula. The results show that the leaching behavior of aluminum and iron ions conformed to the “mixing control” model equation: $“(1 - x)^{-1/3} - 1 + 1/3 \ln(1 - x) = kt + b”$. The apparent activation energies of aluminum and iron ions are 55.5 kJ/mol and 55.8 kJ/mol, respectively. All these indicate that the acid leaching process is controlled by the “mixing control”.

Keywords: high iron content coal gangue; acid leaching; extraction of aluminum and iron ions; acid leaching kinetic



Citation: Kong, D.; Zhou, Z.; Jiang, R.; Song, S.; Feng, S.; Lian, M.

Extraction of Aluminum and Iron Ions from Coal Gangue by Acid Leaching and Kinetic Analyses. *Minerals* **2022**, *12*, 215. <https://doi.org/10.3390/min12020215>

Academic Editors: Carlos Hoffmann Sampaio, Wesley Monteiro Ambros and Bogdan Grigore Cazacliu

Received: 6 January 2022

Accepted: 1 February 2022

Published: 7 February 2022

Publisher's Note: MDPI stays neutral with regard to jurisdictional claims in published maps and institutional affiliations.



Copyright: © 2022 by the authors. Licensee MDPI, Basel, Switzerland. This article is an open access article distributed under the terms and conditions of the Creative Commons Attribution (CC BY) license (<https://creativecommons.org/licenses/by/4.0/>).

1. Introduction

Coal gangue is the waste produced by the coal industry [1], which accounts for 10–20% of the raw coal output [2]. Due to the massive accumulation of coal gangue, it has polluted the atmosphere, water, and soil [3], occupied land, and affected the safety of the ecological environment [4]. The resource utilization of coal gangue is conducive to decreasing its ecological damage and enhancing industrial added value. The common ways to utilize gangue include mine backfilling [5], brick making [6,7], road paving [8], cement making [9], etc. However, these methods cannot make use of coal gangue for high-value-added applications, so it is imperative to research a method of efficient development and comprehensive utilization of coal gangue [10,11].

High-value-added applications of coal gangues include the preparation of molecular sieves [12], the preparation of adsorbents [13], the extraction of elements such as aluminum and silicon [14], and the preparation of products using extracted materials such as Al(OH)₃ [15], Al₂O₃ [16,17], AlCl₃ [18], Al₂(SO₄)₃ [19], polyaluminium chloride [20], Na₂SiO₃, and SiO₂ [21]. Most coal gangues used in these studies have low iron content, so the purity and whiteness of the prepared products are high.

The increase in iron content in coal gangue will increase the probability of iron entering the products, which will affect its application fields, and even make it difficult to carry out fine processing directly [22]. In Liupanshui, Guizhou Province, China, more than 10 million

tons of coal gangue are produced every year, and coupled with years of accumulation, the current amount of coal gangue is more than 180 million tons. The components of coal gangue in this area are different from those in other areas, and its main feature is that it is rich in iron. Therefore, it cannot be used in areas requiring product purity and whiteness.

Generally, aluminum and iron elements from coal gangue can be extracted to prepare $\text{Al}(\text{OH})_3$, Al_2O_3 , Fe_2O_3 , and composite coagulant [23,24]. There are various methods for the extraction of aluminum and iron ions, such as acid leaching and alkali leaching [25–28].

With these methods, the extraction ratios of aluminum and iron elements are affected not only by the process conditions, but also by the kinds of minerals. However, the components of gangue vary from place to place, so these existing technologies cannot be copied and applied directly. Therefore, it is necessary to explore the optimal leaching process conditions.

In this work, the components, phases, morphology, and the thermal–chemical properties of the coal gangue from Liupanshui are analyzed by XRF, XRD, SEM, and TG-DSC, respectively. The suitable process conditions of extracting aluminum and iron ions are obtained. Three control models in the “unreacted core shrinkage model” (USCM) are used to fit the leaching kinetics of aluminum and iron ions in the acid leaching process of hydrochloric acid. The results show that “the mixed control” model can explain the leaching kinetics of coal gangue samples effectively.

2. Experimental Section

2.1. Materials

The coal gangue came from Wangjiazhai Coal Mine of Liupanshui, Guizhou Province, China, which was made into powder of less than 160 mesh. Sulfuric acid and hydrochloric acid were the analytical reagents, from Chongqing Chuandong Chemical Co., Ltd. Chongqing, China.

2.2. Procedure

As shown in Figure 1, the gangue was crushed and passed through a 160-mesh sieve, then calcined at a high temperature for a certain time to obtain the calcined powder; then, the calcined powder was acid-leached by sulfuric acid or hydrochloric acid at the solid:liquid ratio of 1:3.5, at a temperature of 93 °C, and the stirring speed of 1000 r/min for 1–7 h. After the acid leaching had completed, suction filtration, washing, and drying were carried out. According to the quantity of the filter residue and its chemical components, the extraction ratios of aluminum and iron ions were calculated by the following formulas:

$$\text{yield of residue} = (m_2 \div m_1) \times 100\% \quad (1)$$

$$x = [(m_1 \times w_1\% - m_2 \times w_2\%) \div m_1 w_1\%] \times 100\% \quad (2)$$

where “ m_1 ” is the quantity of the calcined powder before leaching, “ m_2 ” is the quantity of the filter residue, “ $w_1\%$ ” is the mass fraction of aluminum or iron ions in the calcined gangue powder, and “ $w_2\%$ ” is the mass fraction of aluminum or iron ions in the filter residue. The compositions of calcined powder before and after acid leaching were detected by XRF, and the concentration of filtrate was calculated accordingly. Then, the USCM was adopted to analyze the leaching kinetics of aluminum and iron ions, and the apparent activation energies were calculated.

A 6100 type X-ray diffraction instrument (XRD, Shimadzu Company, Japan) was used for $\text{CuK}\alpha$ (λ for $\text{K}\alpha = 1.54059 \text{ \AA}$), $2\theta = 3^\circ\text{--}65^\circ$, with a step width of 0.02° . The primary chemical elemental components were determined by a Supermini200 type X-ray fluorescence spectrometer (XRF, Rigaku Company, Tokyo, Japan). The morphology of the products was identified by a Zeiss EVO18-type scanning electron microscope (SEM, Jena, Germany). The thermal–chemical properties of coal gangue were characterized by a SDT–Q600 type thermal analyzer (TG-DSC, TA Company, Boston, MA, USA), and analyses were performed under the air atmosphere at a constant flow rate of 100 mL/min, where

the sensitivity of the microbalance was 0.1 μg , the accuracy of temperature measurement was 0.1 $^{\circ}\text{C}$, and the heating rate was 20 $^{\circ}\text{C}/\text{min}$.

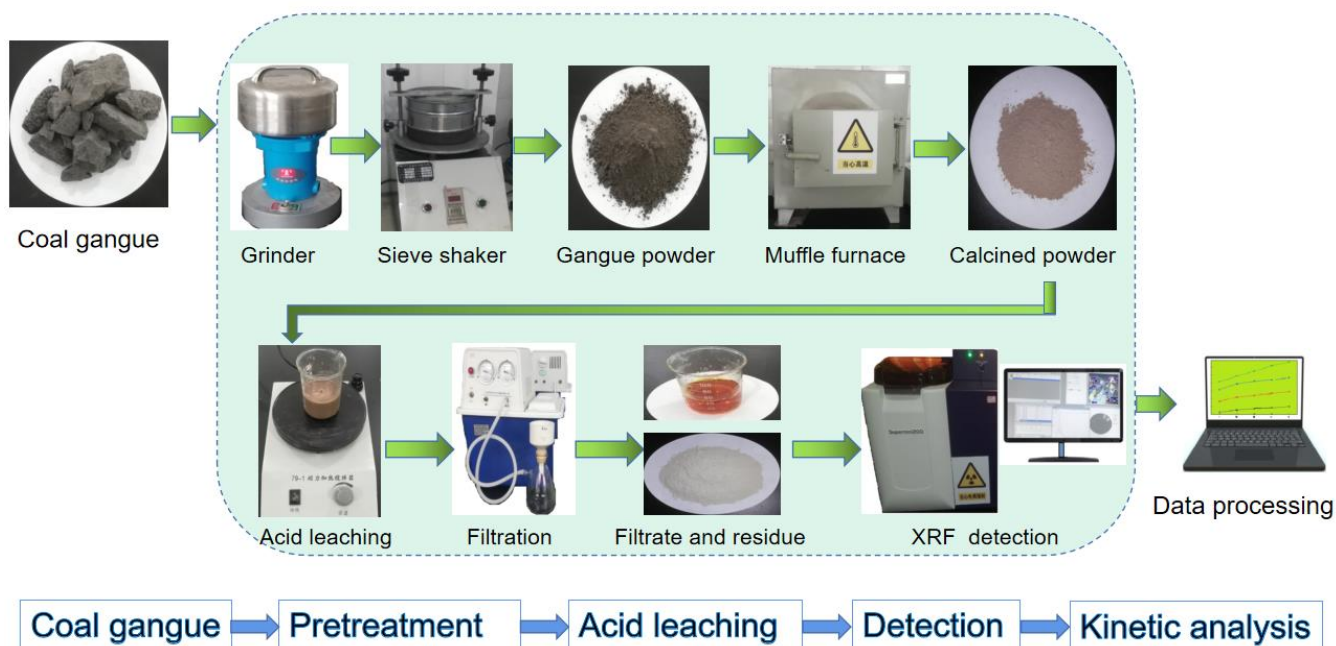


Figure 1. Flow chart of the experiments.

2.3. Instrumentation and Characterization

3. Results and Discussion

3.1. Chemical Components of the Coal Gangue

As shown in Table 1, the contents of SiO_2 , Al_2O_3 , and Fe_2O_3 in the gangue accounted for 75.55% of the total quantity. Compared with the coal gangue in other parts of China, the content of the iron element in the sample is higher, whereas the content of the aluminum element is lower.

Table 1. Main components of the coal gangue.

Components	wt/%
SiO_2	42.18
Al_2O_3	20.43
Fe_2O_3	11.94
CaO	2.95
MgO	1.61
MnO	0.25
P_2O_5	0.30
TiO_2	3.77
S	0.54
K_2O	1.24
Na_2O	0.40
FC and Loss	14.39

3.2. XRD Analysis of the Coal Gangue

As seen from Figure 2, the coal gangue is a multiphase mixture [29], and the main phases in the coal gangue are kaolinite, quartz, brookite, montmorillonite, pyrite, and siderite [30], in which kaolinite and quartz are the main components. As shown in Table 1, the iron content is high, but the peaks of the iron-containing materials are lower, which indicates that the crystallinity of the iron-containing materials is low.

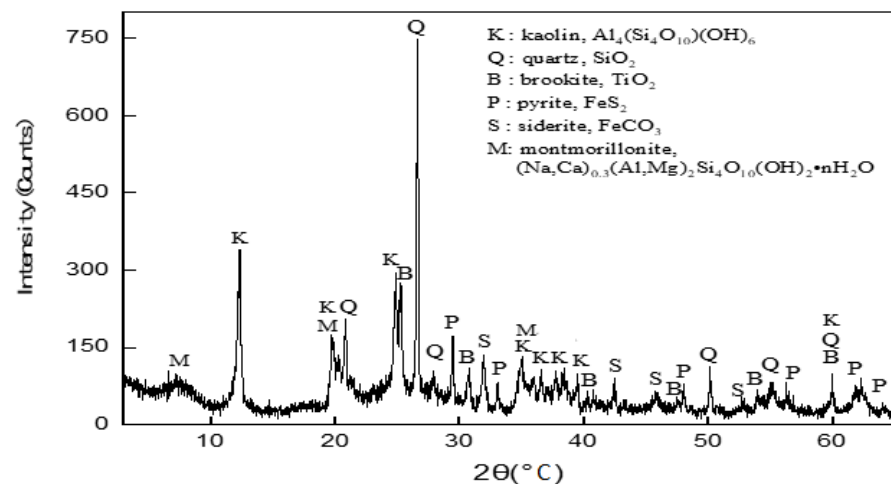


Figure 2. XRD spectrum of coal gangue powder.

3.3. Morphology Analysis of the Coal Gangue

It can be seen from Figure 3 that the coal gangue powders are spherical with an uneven particle size. The maximum particle size is more than 30 μm , whereas the minimum is about 1 μm .

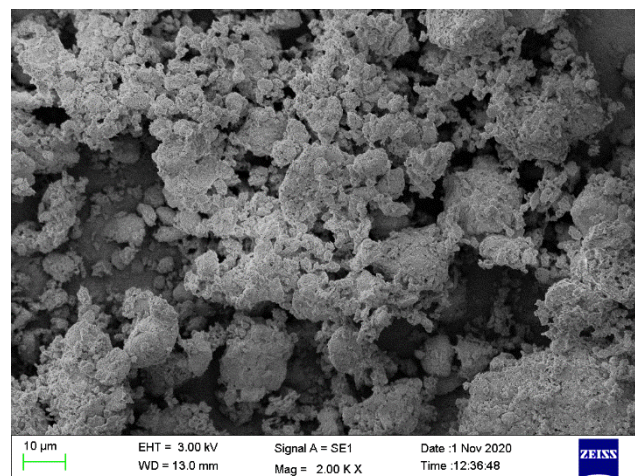


Figure 3. SEM image of raw gangue powders.

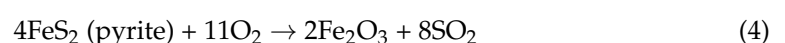
3.4. TG-DSC Analyses of the Coal Gangue

In order to obtain a suitable thermal activation temperature range, the thermal analyses of coal gangue were carried out by TG-DSC. The results are shown in Figure 4.

In Figure 4, the endothermic valley between 100 and 400 $^{\circ}\text{C}$ is mainly caused by the dehydration of water in coal gangue, but the quantity loss is not obvious within this temperature range, which indicates that the content of crystal water in the coal gangue is low. The exothermic peak near 598 $^{\circ}\text{C}$ is mainly caused by the combustion exothermic of coal, pyrite, and other components. When the temperature is higher than 500 $^{\circ}\text{C}$, kaolinite begins to decompose into metakaolin [31,32], which is an endothermic reaction. The equation is as follows:



The combustion of pyrite is an exothermic reaction, and the reaction is as follows:



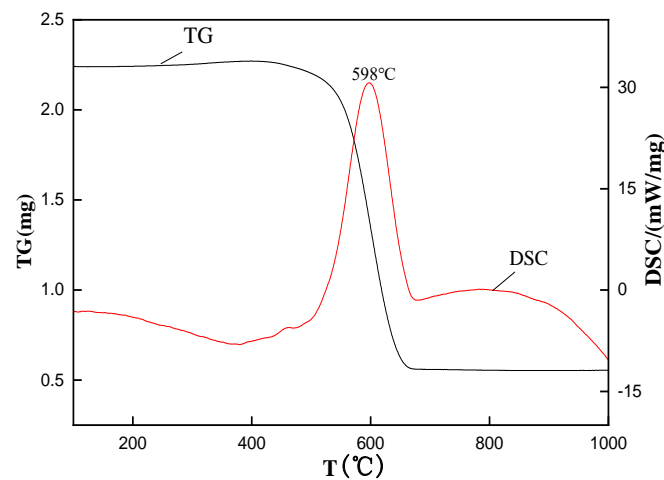
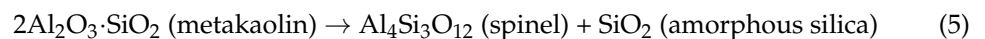


Figure 4. TG – DSC chart of the coal gangue.

Overall, the total heat release is larger than the heat absorption, which exhibits an exothermic peak. On the TG curve, the quantity decreases significantly for the combustion of coal and pyrite which produce CO_2 , SO_2 , H_2O , and other volatile substance products [33]. Meanwhile, siderite is decomposed into Fe_xO_y , CO_2 , or CO , and the volatilizations lead to the quantity loss. When the temperature exceeds 650°C , kaolin, pyrite, siderite, and other substances have basically produced decomposition, so the quantity is almost unchanged. The low exothermic peak near 800°C is formed by the continuous combustion and heat release of the residual coal in the coal gangue [34]. The endothermic valley between 900 and 1000°C is attributed to metakaolin, which is endothermically decomposed into spinel and amorphous silica [35,36]. The main reaction is as follows:



3.5. Phase Analyses of the Calcined Powders at Different Temperatures

As shown in Figure 5, kaolinite and other minerals can be decomposed completely at $600\text{--}800^\circ\text{C}$. Therefore, it is conducive to the activation of minerals and the combustion of coal gangue components when enhancing the temperature appropriately. However, too high a temperature will not only waste energy, but also lead to the transformations of metakaolin and other substances into other phases.

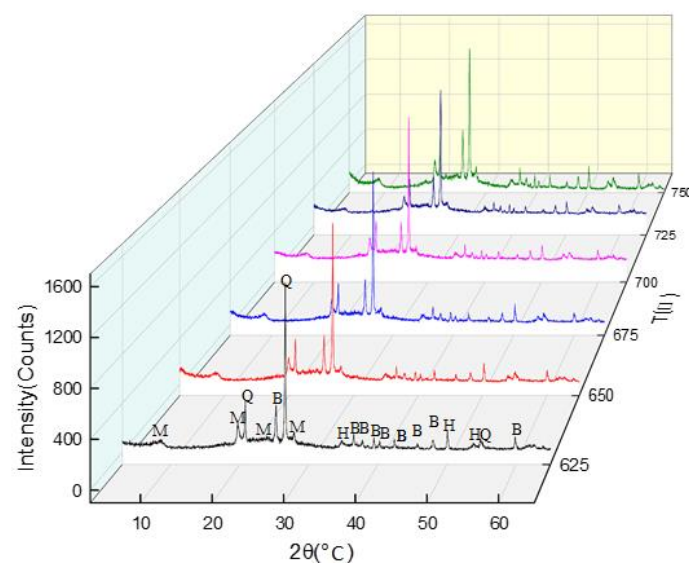


Figure 5. XRD spectra of the calcined powders at different temperatures. H: hematite, Fe_2O_3 .

There are still crystal inert substances such as quartz and brookite, and the main contents of these substances are silicon and titanium. The gangue rich in aluminum and iron has been transformed into a highly active amorphous state [37], including amorphous Al_2O_3 and SiO_2 . Therefore, coal gangue can be activated in the range of 625–750 °C.

3.6. Analyses of the Leaching Effects with Different Acids

Two aliquots with masses of 10 g coal gangue powders were calcined at 750 °C for 2 h, and then the powders were leached by 3.0 mol/L sulfuric acid and 6.0 mol/L hydrochloric acid, respectively. The solid:liquid ratio was 1:3.5, and the whole process was stirred at 93 °C. After the acid leaching reactions, the solid:liquid mixtures were filtered, washed, and dried. After that, the quantities of the filter residues were weighed to obtain the yields of the residues. The results are presented in Figure 6.

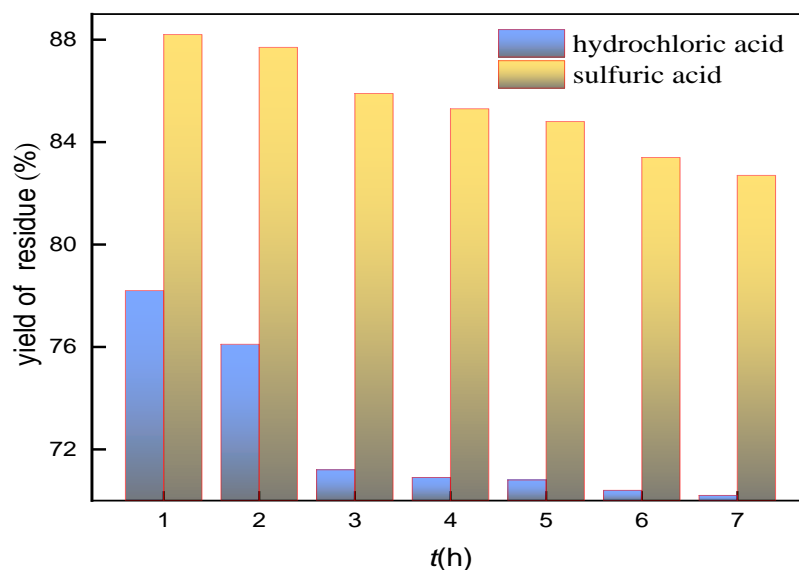


Figure 6. The effect of acid leaching time on the yield of residue.

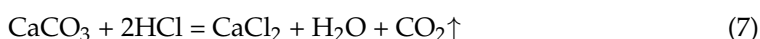
As seen from Figure 6, the yields of residue decrease with the extension of time. The yields of residue by sulfuric acid leaching are obviously higher than that of hydrochloric acid.

Hydrochloric acid is a common industrial waste acid, although its demand is not as high as sulfuric acid; therefore, using hydrochloric acid could provide a certain reference for industrial production. In addition, coal gangue contains calcium ions, and adding sulfuric acid can easily produce CaSO_4 . The equation is as follows:



CaSO_4 is a substance which is slightly soluble in water. It is easy to cover the surface of the particles and affect the diffusion of ions, which is not conducive to metal ion leaching.

The reaction of hydrochloric acid with CaCO_3 produces CaCl_2 , which is soluble in water and conducive to the dissolution of other ions. The equation is as follows:



In fact, hydrochloric acid is used very actively in the field of hydrometallurgy, which is used to leach iron or aluminum from coal ash [38], fly ash [39], bauxite [40,41], red mud [42], and coal gangue [43,44]. As can be seen from the results in Figure 6, the effect of hydrochloric acid is significantly better than that of sulfuric acid, so hydrochloric acid was chosen, and the time can be 3–7 h. In order to leach the gangue fully and save energy, the leaching time was determined to be 4 h.

The coal gangue was calcined at 750 °C for 2 h, and after leaching, the phase analyses of the two acid-leached residues are shown in Figure 7.

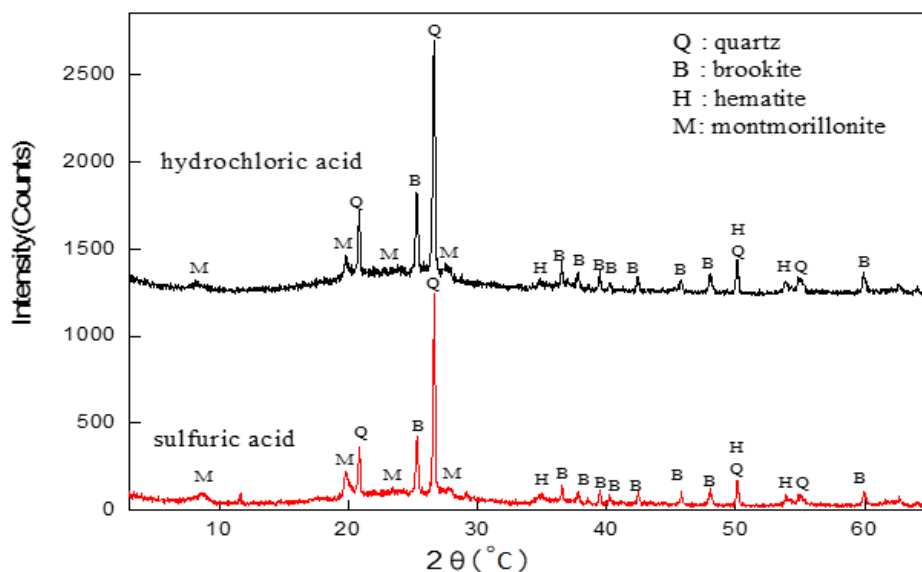


Figure 7. XRD spectra of the filter residue after acid leaching with different acids for 6 h.

As shown in Figure 7, the diffraction peaks of the intensity of the quartz and brookite in the filter residue of the leached hydrochloric acid are higher than those of the sulfuric acid, and because more aluminum and iron ions are dissolved by hydrochloric acid, the higher the contents of the remaining quartz and brookite.

3.7. Effects of Calcination Temperature on the Yield of Residue

After the reactions, the reduction quantity was calculated. The results are shown in Figure 8. When the calcination temperature was between 550 and 700 °C, the yield tended to be stable, and the minimum yield was at 675 °C. However, when the calcination temperature was raised to 700–750 °C, the yield increased, indicating that the calcined temperature affects the activity of aluminum and iron ions. In order to activate the aluminum and iron components, as well as remove carbon as much as possible, 675 °C was selected as the proper calcination temperature.

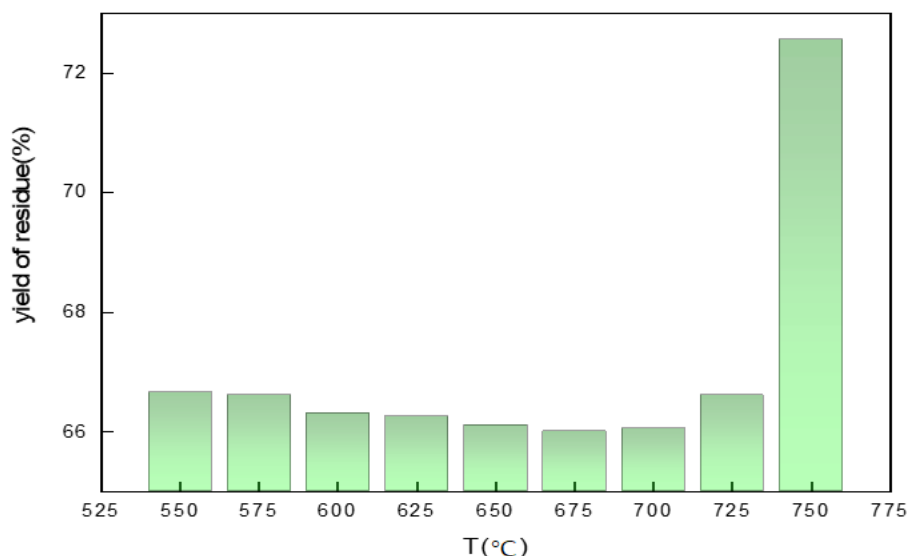


Figure 8. Effects of calcination temperature on the yield of residue.

3.8. Effect of Calcination Time on the Yield of Residue

The coal gangue powders were calcined at 675 °C for 30 min, 45 min, 60 min, 75 min, 90 min, 105 min, 120 min, and 135 min. The other conditions are the same as above, and the results are shown in Figure 9.

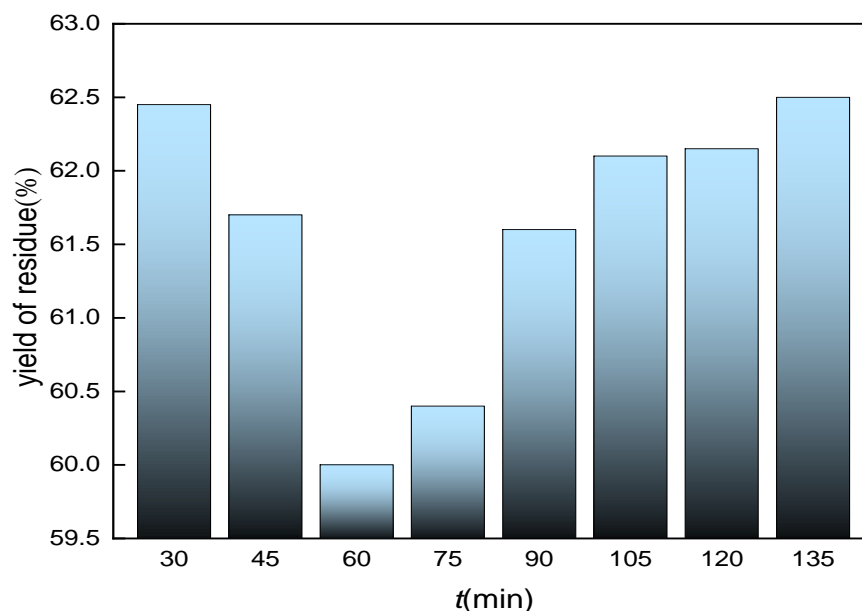


Figure 9. Effect of different calcination time on the yield of residue at 675 °C.

As shown in Figure 9, when the calcination time was 30–60 min, the yield of residue decreased with the extension of time because the kaolinite, siderite, pyrite, etc., in the coal gangue underwent chemical reactions to produce a large amount of amorphous Al_2O_3 , SiO_2 , and Fe_xO_y , which improved the activity of the calcined powder, thereby decreasing the yield. When the time was extended more than 60 min, the activity of the calcined powder decreased, which led to the increased yield. Therefore, the calcination time was determined to be 1 h. The components of the acid-leached residue are displayed in Table 2.

Table 2. Main components of the residue.

Components	wt/%
SiO_2	76.95
Al_2O_3	10.37
Fe_2O_3	1.00
CaO	0.05
MgO	0.22
TiO_2	6.22
MnO	0.04
P_2O_5	0.06
S	0.01
K_2O	1.01
Na_2O	0.38
FC and others	3.69

As seen from Table 2, the primary acid-leached filter residue contained 76.95% of SiO_2 and 10.37% of Al_2O_3 . According to the calculations, 91% of iron ions and 66% of aluminum ions have been leached, and the concentration of AlCl_3 is 94.26 g/L and that of FeCl_3 is 73.13 g/L. The mixed liquid containing aluminum and iron can be used to prepare composite coagulants, or to prepare alumina and iron oxide by a step precipitation

method. The residue is mainly silicon- and titanium-containing material, which can be used to prepare other products such as zeolites [45], silica, TiO_2 , etc.

3.9. Morphology Analysis of Filter Residue

As shown in Figure 10, the particle sizes of the acid-leached filter residues are smaller than that of the ore coal gangue powder, and the largest particle size is about $20\ \mu\text{m}$. It can also be seen that due to the leaching of iron and aluminum ions, the residue particles become loose, showing flakes and crumbs.

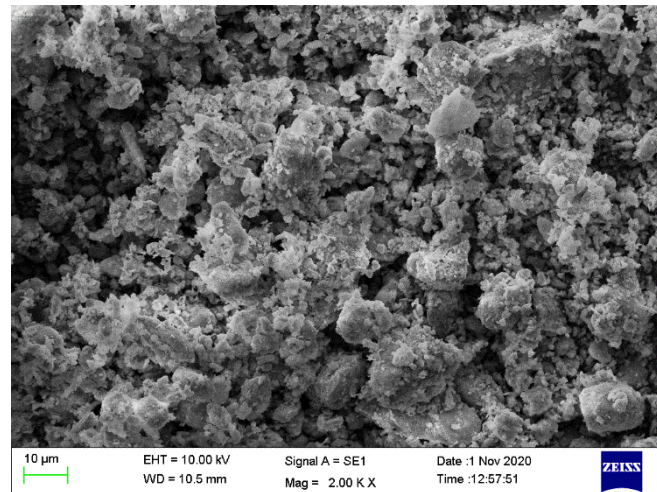


Figure 10. SEM image of the residue.

3.10. Analysis of Leaching Kinetics

The components of coal gangue are very complex, in which iron oxide comes from FeCO_3 and pyrite, as well as other amorphous iron compounds; aluminum primarily comes from amorphous alumina produced by the decomposition of kaolinite. In the leaching process, acid molecules diffuse into the voids or cracks of quartz or amorphous SiO_2 , and then react with aluminum and iron oxides. With the reactions, products come out from the residual solid layers, and the reaction interface continues to shrink to the core of the mineral particles. Simultaneously, the residual solid layer continues to thicken, and some solid layers may form debris and peel off under stirring. Therefore, the “USCM” is used to describe the leaching kinetics of aluminum and iron ions [46–48].

The reaction model of the leaching process is shown in Figure 11.

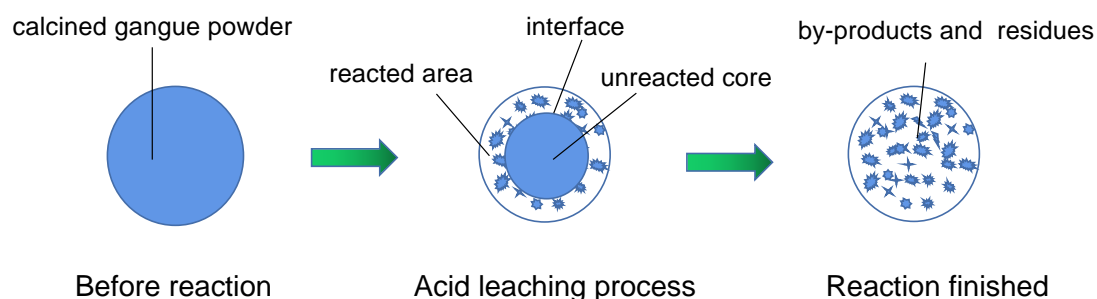


Figure 11. Schematic diagram of acid leaching process.

Assuming that the calcined coal gangue powder particles are approximately spherical, and the leaching process is controlled by the “solid film diffusion control”, the leaching kinetic equation is as follows:

$$1 - 2/3x - (1 - x)^{2/3} = k_1 t + b_1 \quad (8)$$

If the control step is the “interface chemical reaction control”, the equation is as follows:

$$1 - (1 - x)^{1/3} = k_2t + b_2 \tag{9}$$

When the leaching process is jointly controlled by the “solid film diffusion control” and the “interface chemical reaction control” together, it is called the “mixing control”, and the equation is [49]:

$$(1 - x)^{-1/3} - 1 + 1/3\ln(1 - x) = k_3t + b_3 \tag{10}$$

where “ k_1 ” is the solid–liquid diffusion rate constant, “ k_2 ” is the rate constant of interfacial chemical reaction, “ k_3 ” is the rate constant of mixing control reaction, “ x ” is the leaching ratio, “ t ” is the leaching time, and “ b_1, b_2 and b_3 ” are the constant terms.

In order to determine the control type of hydrochloric acid leaching reactions, the extraction ratios of aluminum and iron ions changing with temperature and time were assessed. The temperature increased from 303.15 K to 363.15 K with a step of 20 K, the time was from 10 min to 5 h, the H^+ concentration is 6 mol/L, and the stirring speed was 1000 r/min. Since the contents of calcium and magnesium ions in coal the gangue were very low (Cao 0.05%, MgO 0.22%), and TiO_2 (6.22%) did not react with dilute hydrochloric acid, we ignored the effects of calcium, magnesium, and titanium ions on leaching. The results are shown in Figures 12 and 13.

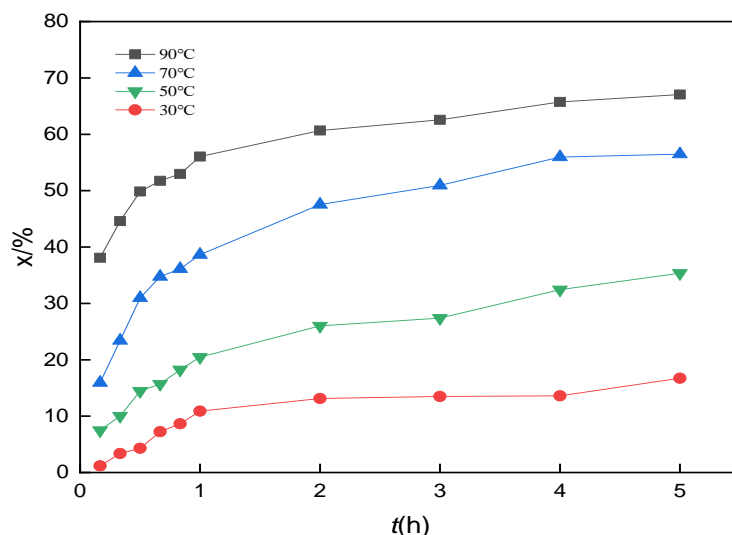


Figure 12. Effects of temperature on the extraction ratios of aluminum ions.

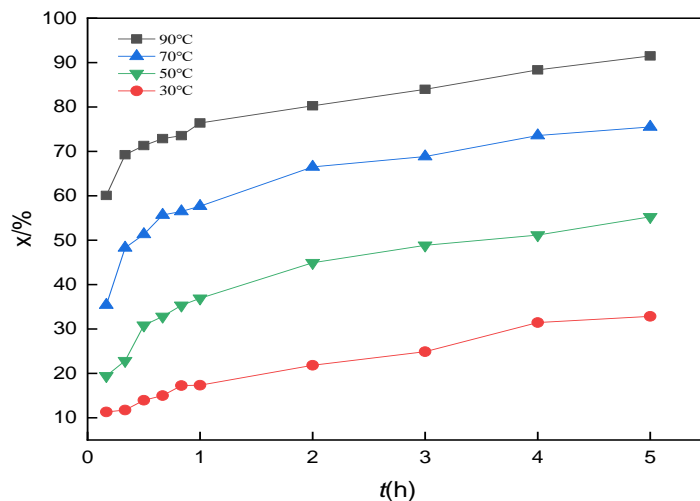


Figure 13. Effects of temperature on the extraction ratios of iron ions.

A trial method is used to substitute the obtained results into the kinetic equations of the different control steps, plotting $1 - 2/3x - (1 - x)^{2/3}$, $1 - (1 - x)^{1/3}$ and $(1 - x)^{-1/3} - 1 + 1/3\ln(1 - x)$ versus t , respectively, and then using these three models to fit the obtained data linearly. The results of aluminum ions are shown in Figures 14–16, and so the iron ions are shown in Figures 17–19.

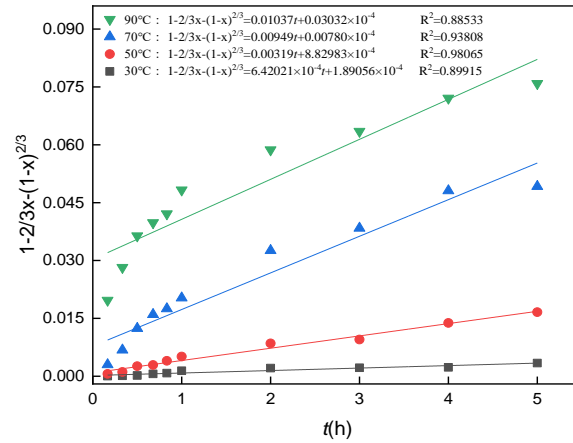


Figure 14. Relationships between $1 - 2/3x - (1 - x)^{2/3}$ and time of aluminum ions.

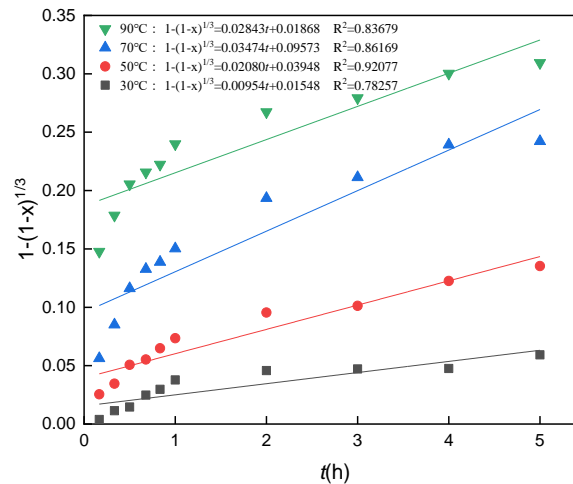


Figure 15. Relationships between $1 - (1 - x)^{1/3}$ and time of aluminum ions.

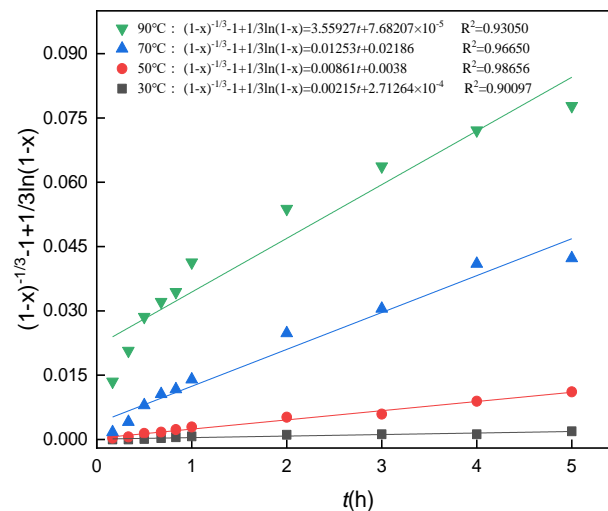


Figure 16. Relationships between $(1 - x)^{-1/3} - 1 + 1/3\ln(1 - x)$ and time of aluminum ions.

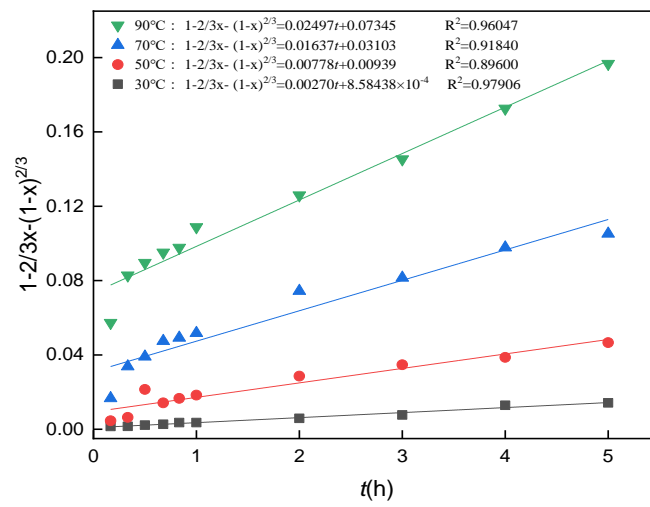


Figure 17. Relationships between $1 - 2/3x - (1 - x)^{2/3}$ and time of iron ions.

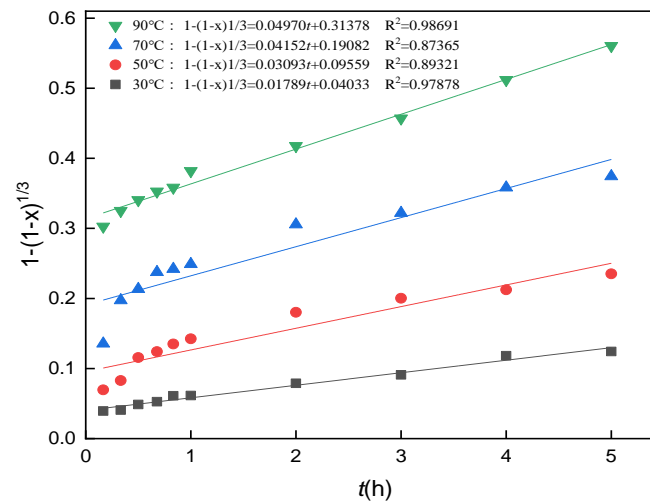


Figure 18. Relationships between $1 - (1 - x)^{1/3}$ and time of iron ions.

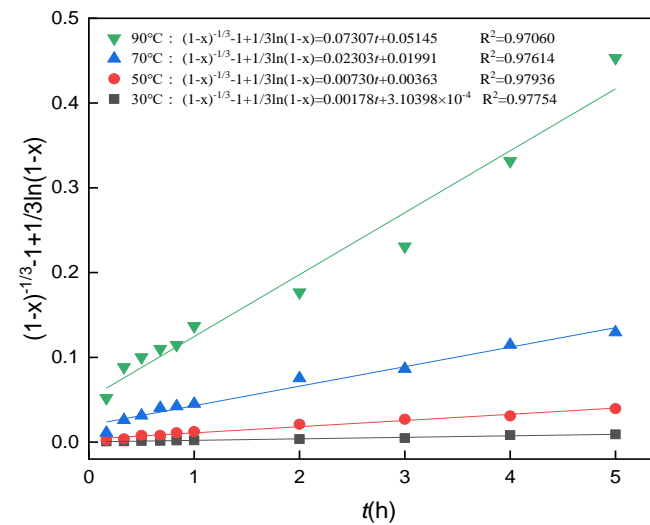


Figure 19. Relationships between $(1 - x)^{-1/3} - 1 + 1/3\ln(1 - x)$ and time of iron ions.

As can be seen from the fitting equations and the R² values of these three mathematical models, whether aluminum ion leaching or iron ion leaching, the R² values of the mixing

control equation at 30 °C, 50 °C, 70 °C, and 90 °C were all better than that of single “solid film diffusion control” or “interface chemical reaction control”, and were all closer to 1. Therefore, hydrochloric acid leaching aluminum and iron ions kinetic equations from the calcined coal gangue powder are all accord with the “mixing control” models.

3.11. Calculation of the Apparent Activation Energy

To obtain the activation energies of aluminum and iron ions extraction under hydrochloric acid leaching conditions, the Arrhenius formula was used to determine the apparent activation energies of the leaching experiments. According to the Arrhenius formula:

$$k = Ae^{-Ea/RT} \tag{11}$$

$$\ln k = -Ea/RT + \ln A \tag{12}$$

where “k” is the apparent reaction rate constant, “Ea” is the apparent activation energy, kJ/mol, “R” is the molar gas constant, 8.314 J/(mol K), and “A” is a constant. The fitting curves of $\ln k - 1/T$ of aluminum and iron ions are shown in Figures 20 and 21. The apparent activation energies can be calculated from the slope of the fitting equations based on Arrhenius formula, where the slope is $-Ea/RT$ and the intercept is $\ln A$.

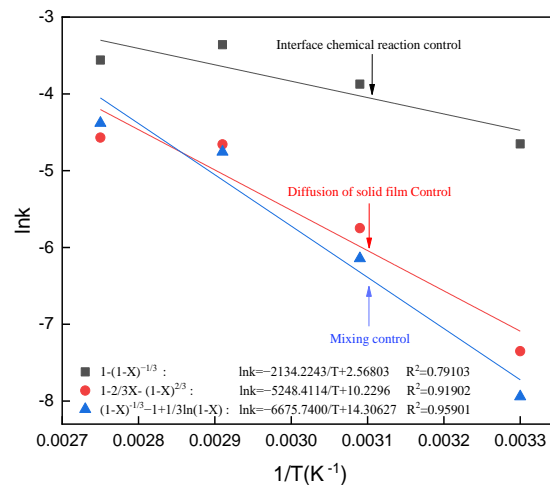


Figure 20. Curves of $\ln k - 1/T$ to aluminum ions.

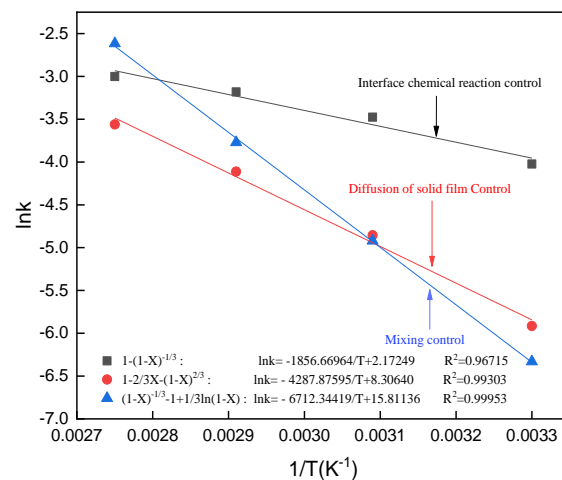


Figure 21. Curves of $\ln k - 1/T$ to iron ions.

As seen from Figure 20, the correlation fitting degree of the $\ln k - 1/T$ curve ($R^2 = 0.95901$) obtained from the “mixing control” fitting is significantly better than that of the diffusion

of solid film control ($R^2 = 0.91902$) and interfacial chemical reaction control ($R^2 = 0.79103$). Similarly, the correlation coefficient R^2 of the iron ions fitting equation using the “mixing control” model is also better than that of the other two models (Figure 21), which further indicates that the leaching ratios of aluminum and iron ions from calcined coal gangue powder by hydrochloric acid leaching are both affected by the “mixing control”.

According to Figures 20 and 21, we can derive:

$$\ln k_{(Al)} = -6675.7400/T + 14.30627 \quad (13)$$

$$\ln k_{(Fe)} = -6712.34419/T + 15.81136 \quad (14)$$

$$E_{a(Al)} = 6675.7400R = 55.5 \times 10^3 \text{ J/mol} = 55.5 \text{ kJ/mol} \quad (15)$$

$$E_{a(Fe)} = 6712.3442R = 55.8 \times 10^3 \text{ J/mol} = 55.8 \text{ kJ/mol} \quad (16)$$

The apparent activation energies of aluminum and iron ion leaching are 55.5 kJ/mol and 55.8 kJ/mol, respectively.

4. Conclusions

In the study of extracting aluminum and iron ions from coal gangue, the proper conditions were obtained when the gangue powder was less than 160 mesh, the calcination temperature was 675 °C, the time was 60 min, and the calcined coal gangue was leached by 6 mol/L hydrochloric acid at 93 °C for 4 h, where the leaching ratio of iron ions was 91% and that of aluminum ions was 66%.

The process of leaching aluminum and iron ions from the calcined coal gangue powder with hydrochloric acid conforms to the kinetic model: $(1 - x)^{-1/3} - 1 + 1/3 \ln(1 - x) = k_3 t + b_3$. According to the Arrhenius equation, the apparent activation energies of the leaching reactions of aluminum and iron are 55.5 kJ/mol and 55.8 kJ/mol, respectively. The leaching process of aluminum and iron ions are controlled by the “mixing control”.

Author Contributions: D.K.: Literature search, Conceptualization, Methodology, Investigation, Visualization, Experiment, Data analysis; Writing—Original Draft, Writing—Review and Editing; R.J.: Investigation, Data analysis; Writing—Review and Editing; Z.Z.: Investigation, Writing—Review and Editing; S.S.: Investigation, Data analysis; Writing—Review and Editing; S.F.: Investigation, Writing—Review and Editing; M.L.: Writing—Review and Editing. All authors have read and agreed to the published version of the manuscript.

Funding: This research was funded by Guizhou Provincial Science and Technology Department: 2018]1142 and [2018]1415, Guizhou Provincial Education Department: [2017]054, Liupanshui City Science and Technology Foundation: 52020-2019-05-17.

Data Availability Statement: The study did not report any data.

Acknowledgments: The study was financially supported by Guizhou Provincial Education Department’s Scientific and Technological Innovation Team Project (NO. [2017]054), the Guizhou Science and Technology Foundation Project (NO. [2018]1142 and [2018]1415), and the Liupanshui City Science and Technology Foundation (NO. 52020-2019-05-17).

Conflicts of Interest: The authors declare no conflict of interest.

References

1. Ma, H.Q.; Zhu, H.G.; Wu, C.; Chen, H.Y.; Sun, J.W.; Liu, J.Y. Study on compressive strength and durability of alkali-activated coal gangue-slag concrete and its mechanism. *Powder Technol.* **2020**, *368*, 112–124. [[CrossRef](#)]
2. Huang, G.D.; Ji, Y.S.; Li, J.; Hou, Z.H.; Dong, Z.C. Improving strength of calcinated coal gangue geopolymer mortars via increasing calcium content. *Construct. Build. Mater.* **2018**, *166*, 760–768. [[CrossRef](#)]
3. Yang, F.L.; Yang, Y.; Li, G.K.; Sang, N. Heavy metals in soil from gangue stacking areas increases children health risk and causes developmental neurotoxicity in zebrafish larvae. *Sci. Total Environ.* **2021**, *794*, 148629. [[CrossRef](#)] [[PubMed](#)]
4. Gomo, M.; Vermeulen, D. Hydrogeochemical characteristics of a flooded underground coal mine groundwater system. *J. Afr. Earth. Sci.* **2014**, *92*, 68–75. [[CrossRef](#)]

5. Li, M.; Zhang, J.X.; Li, A.L.; Zhou, N. Reutilisation of coal gangue and fly ash as underground back fill materials for surface subsidence control. *J. Clean. Prod.* **2020**, *254*, 120113. [[CrossRef](#)]
6. Xu, H.L.; Song, W.J.; Cao, W.B.; Shao, G.; Lu, H.X.; Yang, D.Y.; Chen, D.; Zhang, R. Utilization of coal gangue for the production of brick. *J. Mater. Cycles Waste Manag.* **2017**, *19*, 1270–1278. [[CrossRef](#)]
7. Xu, B.H.; Liu, Q.F.; Ai, B.; Ding, S.L.; Frost, R.L. Thermal decomposition of selected coal gangue. *J. Therm. Anal. Calorim.* **2018**, *131*, 1–10. [[CrossRef](#)]
8. Guan, J.; Lu, M.; Yao, X.H.; Wang, Q.; Wang, D.C.; Yang, B.; Liu, H. An experimental study of the road performance of cement stabilized coal gangue. *Crystals* **2021**, *11*, 993. [[CrossRef](#)]
9. Zhou, M.; Dou, Y.W.; Zhang, Y.Z.; Zhang, Y.Q.; Zhang, B.Q. Effects of the variety and content of coal gangue coarse aggregate on the mechanical properties of concrete. *Construct. Build. Mater.* **2019**, *220*, 386–395. [[CrossRef](#)]
10. Yang, J.; Zhang, X.; Liu, Y.Q.; Ma, H.W.; Feng, W.W.; Zeng, C. Synthesis of ultrafine silica powder using the silica source alkali-leached from coal gangue. *Integr. Ferroelectr.* **2015**, *161*, 10–17. [[CrossRef](#)]
11. Wu, R.D.; Dai, S.B.; Jian, S.W.; Huang, J.; Tan, H.B.; Li, B.D. Utilization of solid waste high-volume calcium coal gangue in autoclaved aerated concrete: Physico-mechanical properties, hydration products and economic costs. *J. Clean. Prod.* **2021**, *278*, 123416. [[CrossRef](#)]
12. Bu, N.J.; Liu, X.M.; Song, S.L.; Liu, J.H.; Yang, Q.; Li, R.; Zheng, F.; Yan, L.; Zhen, Q.; Zhang, J. Synthesis of NaY zeolite from coal gangue and its characterization for lead removal from aqueous solution. *Adv. Powder Technol.* **2020**, *31*, 2699–2710. [[CrossRef](#)]
13. Gao, Y.; Huang, J.D.; Li, M.; Dai, Z.R.; Jiang, R.L.; Zhang, J.X. Chemical modification of combusted coal gangue for U(VI) adsorption: Towards a waste control by waste strategy. *Sustainability* **2021**, *13*, 8421. [[CrossRef](#)]
14. Han, L.; Ren, W.; Wang, B.; He, X.; Ma, L.; Huo, Q.; Wang, J.; Bao, W.; Chang, L. Extraction of SiO₂ and Al₂O₃ from coal gangue activated by supercritical water. *Fuel* **2019**, *253*, 1184–1192. [[CrossRef](#)]
15. Tang, Z.H. Preparation of nanometer Al(OH)₃ powder using coal gangue by polyacrylamide dispersant-carbonization method. *Adv. Mater. Res.* **2011**, *160–162*, 307–313. [[CrossRef](#)]
16. Dong, L.; Liang, X.; Song, Q.; Gao, G.; Song, L.; Shu, Y.; Shu, X. Study on Al₂O₃ extraction from activated coal gangue under different calcination atmospheres. *J. Therm. Sci.* **2017**, *26*, 570–576. [[CrossRef](#)]
17. Guo, Y.X.; Zhao, Q.; Yan, K.Z.; Cheng, F.Q.; Lou, H.H. Novel process for alumina extraction via the coupling treatment of coal gangue and bauxite red mud. *Ind. Eng. Chem. Res.* **2014**, *53*, 4518–4521. [[CrossRef](#)]
18. Guo, Y.X.; Lv, H.B.; Yang, X.; Cheng, F.Q. AlCl₃·6H₂O recovery from the acid leaching liquor of coal gangue by using concentrated hydrochloric impouring. *Sep. Purif. Technol.* **2015**, *151*, 177–183. [[CrossRef](#)]
19. Cheng, Y.; Hongqiang, M.; Hongyu, C.; Jiabin, W.; Jing, S.; Zonghui, L.; Mingkai, Y. Preparation and characterization of coal gangue geopolymers. *Construct. Build. Mater.* **2018**, *187*, 318–326. [[CrossRef](#)]
20. Wang, R.G.; Yun, L.X. Preparation and wastewater treatment of polymeric aluminum chloride from coal gangue. *Adv. Mater. Res.* **2012**, *518–523*, 780–783. [[CrossRef](#)]
21. Zhang, S.; Zhang, N.; Zhao, W.; Lan, D.; Hao, G.; Yi, X.; Yang, Z.; Hu, J.; He, W.; Liu, Y.; et al. Green preparation of hierarchical porous C/SiO_x composites from coal gangue as anodes for Li-ion batteries. *Solid State Ionics* **2021**, *371*, 115772. [[CrossRef](#)]
22. Zhou, L.; Zhou, H.J.; Hu, Y.X.; Yan, S.; Yang, J.L. Adsorption removal of cationic dyes from aqueous solutions using ceramic adsorbents prepared from industrial waste coal gangue. *J. Environ. Manag.* **2019**, *234*, 245–252. [[CrossRef](#)] [[PubMed](#)]
23. Li, J.F.; Li, J.G.; Liu, X.Y.; Du, Z.P.; Cheng, F.Q. Effect of silicon content on preparation and coagulation performance of poly-silicic-metal coagulants derived from coal gangue for coking wastewater treatment. *Sep. Purif. Technol.* **2018**, *202*, 149–156. [[CrossRef](#)]
24. Luo, K.J.; Ren, G.M. Coagulant prepared by gangue and its application in treatment of coal washing wastewater. *Adv. Mater. Res.* **2010**, *142*, 270–273. [[CrossRef](#)]
25. Xiao, J.; Li, F.; Zhong, Q.; Bao, H.; Wang, B.; Huang, J.; Zhang, Y. Separation of aluminum and silica from coal gangue by elevated temperature acid leaching for the preparation of alumina and SiC. *Hydrometallurgy* **2015**, *155*, 118–124. [[CrossRef](#)]
26. Yang, Q.; Zhang, F.; Deng, X.; Guo, H.; Zhang, C.; Shi, C.; Zeng, M. Extraction of alumina from alumina rich coal gangue by a hydro-chemical process. *Roy. Soc. Open Sci.* **2020**, *7*, 192132. [[CrossRef](#)]
27. Johnston, C.J.; Pepper, R.A.; Martens, W.N.; Couperthwaite, S. Improvement of aluminium extraction from low-grade kaolinite by iron oxide impurities: Role of clay chemistry and morphology. *Miner. Eng.* **2022**, *176*, 107346. [[CrossRef](#)]
28. Remya, P.N.; Kazantzis, N.K.; Emmert, M.H. Selective process steps for the recovery of scandium from jamaican bauxite residue (red mud). *ACS Sustain. Chem. Eng.* **2018**, *6*, 1478–1488.
29. Ma, H.Q.; Yi, C.; Zhu, H.G.; Dong, Z.C.; Chen, H.Y.; Wang, J.X.; Li, D.Y. Compressive strength and durability of coal gangue aggregate concrete. *Mater. Rep.* **2018**, *32*, 2390–2395.
30. Zhang, M.S.; Xiao, L.W. Preparation of a gangue-based X-type zeolite molecular sieve as a multiphase fenton catalyst and its catalytic performance. *ACS Omega* **2021**, *6*, 18414–18425. [[CrossRef](#)]
31. Zhang, Y.Y.; Zhang, Z.Z.; Zhu, M.M.; Cheng, F.Q.; Zhang, D.K. Decomposition of key minerals in coal gangues during combustion in O₂/N₂ and O₂/CO₂ atmospheres. *Appl. Therm. Eng.* **2019**, *148*, 977–983. [[CrossRef](#)]
32. Gasparini, E.; Tarantino, S.; Ghigna, P.; Riccardi, M.P.; Cedillo-González, E.I.; Siligardi, C.; Zema, M. Thermal dehydroxylation of kaolinite under isothermal conditions. *Appl. Clay Sci.* **2013**, *80–81*, 417–425. [[CrossRef](#)]

33. Zhang, Y.Y.; Ge, X.L.; Nakano, J.; Liu, L.L.; Wang, X.D.; Zhang, Z.T. Pyrite transformation and sulfur dioxide release during calcination of coal gangue. *RSC Adv.* **2014**, *4*, 42506–42513. [[CrossRef](#)]
34. Xie, M.Z.; Liu, F.Q.; Zhao, H.L.; Ke, C.Y.; Xu, Z.Q. Mineral phase transformation in coal gangue by high temperature calcination and high-efficiency separation of alumina and silica minerals. *J. Mater. Res. Technol.* **2021**, *14*, 2281–2288. [[CrossRef](#)]
35. Ptáček, P.; Šoukal, F.; Opravil, T.; Nosková, M.; Havlica, J.; Brandštetr, J. The kinetics of Al-Si spinel phase crystallization from calcined kaolin. *J. Solid State Chem.* **2010**, *183*, 2565–2569. [[CrossRef](#)]
36. Kenne Dikko, B.B.; Elimbi, A.; Cyr, M.; Dika Manga, J.; Tchakoute Kouamo, H. Effect of the rate of calcination of kaolin on the properties of metakaolin-based geopolymers. *J. Asian Ceram. Soc.* **2015**, *42*, 130–138. [[CrossRef](#)]
37. Cao, Z.; Cao, Y.D.; Dong, H.J.; Zhang, J.S.; Sun, C.B. Effect of calcination condition on the microstructure and pozzolanic activity of calcined coal gangue. *Int. J. Miner. Process.* **2016**, *146*, 23–28. [[CrossRef](#)]
38. Valeev, D.; Kunilova, I.; Shoppert, A.; Salazar-Concha, C.; Kondratiev, A. High-pressure HCl-leaching of coal ash to extract Al into a chloride solution with further use as a coagulant for water treatment. *J. Clean. Prod.* **2020**, *276*, 123206. [[CrossRef](#)]
39. Valeev, D.; Mikhailova, A.; Atmadzhidi, A. Kinetics of iron extraction from coal fly ash by hydrochloric acid leaching. *Metals* **2018**, *8*, 533. [[CrossRef](#)]
40. Valeev, D.V.; Lainer, Y.A.; Mikhailova, A.B.; Dorofievich, I.V.; Zheleznyi, M.V.; Gol'dberg, M.A. Reaction of bauxite with hydrochloric acid under autoclave conditions. *Metallurgist* **2016**, *60*, 204–211. [[CrossRef](#)]
41. Valeev, D.V.; Lainer, Y.A.; Pak, V.I. Autoclave leaching of boehmite-kaolinite bauxites by hydrochloric acid. *Inorg. Mater. Appl. Res.* **2016**, *7*, 272–277. [[CrossRef](#)]
42. Zinoveev, D.; Grudinsky, P.; Zhiltsova, E.; Grigoreva, D.; Volkov, A.; Dyubanov, V.; Petelin, A. Research on high-pressure hydrochloric acid leaching of scandium, aluminum and other valuable components from the non-magnetic tailings obtained from red mud after iron removal. *Metals* **2021**, *11*, 469. [[CrossRef](#)]
43. Cheng, F.; Cui, L.; Miller, J.D.; Wang, X. Aluminum leaching from calcined coal waste using hydrochloric acid solution. *Miner. Process. Extr. Metall. Rev.* **2012**, *33*, 391–403. [[CrossRef](#)]
44. Zhang, L.; Wang, H.; Li, Y. Research on the extract Al_2O_3 from coal gangue. *Adv. Mater. Res.* **2012**, *524–527*, 1947–1950. [[CrossRef](#)]
45. Kong, D.S.; Jiang, R.L. Preparation of NaA zeolite from high iron and quartz contents coal gangue by acid leaching-alkali melting activation and hydrothermal synthesis. *Crystals* **2021**, *11*, 1198. [[CrossRef](#)]
46. Gui, Q.H.; Khan, M.I.; Wang, S.X.; Zhang, L.B. The ultrasound leaching kinetics of gold in the thiosulfate leaching process catalysed by cobalt ammonia. *Hydrometallurgy* **2020**, *196*, 105426. [[CrossRef](#)]
47. Dickinson, C.F.; Heal, G.R. Solid-liquid diffusion controlled rate equations. *Thermochim. Acta* **1999**, *340*, 89–103. [[CrossRef](#)]
48. Rao, S.; Yang, T.; Zhang, D.; Liu, W.; Chen, L.; Hao, Z.; Xiao, Q.; Wen, J. Leaching of low grade zinc oxide ores in NH_4Cl-NH_3 solutions with nitrilotriacetic acid as complexing agents. *Hydrometallurgy* **2015**, *158*, 101–106. [[CrossRef](#)]
49. Valeev, D.; Pankratov, D.; Shoppert, A.; Sokolov, A.; Kasikov, A.; Mikhailova, A.; Salazar-Concha, C.; Rodionov, I. Mechanism and kinetics of iron extraction from high silica boehmite-kaolinite bauxite by hydrochloric acid leaching. *Trans. Nonferrous Met. Soc. China* **2021**, *31*, 3128–3149. [[CrossRef](#)]